BE/APH161 – PHYSICAL BIOLOGY OF THE CELL

Rob Phillips
Applied Physics and Bioengineering
California Institute of Technology

TWO-COMPONENT SIGNAL TRANSDUCTION

- Next few slides are courtesy of Michael Laub (MIT) and Mark Goulian (Upenn) – experts in the quantitative dissection of signaling networks.
- This figure shows the generic features of the two-component signal transduction systems.

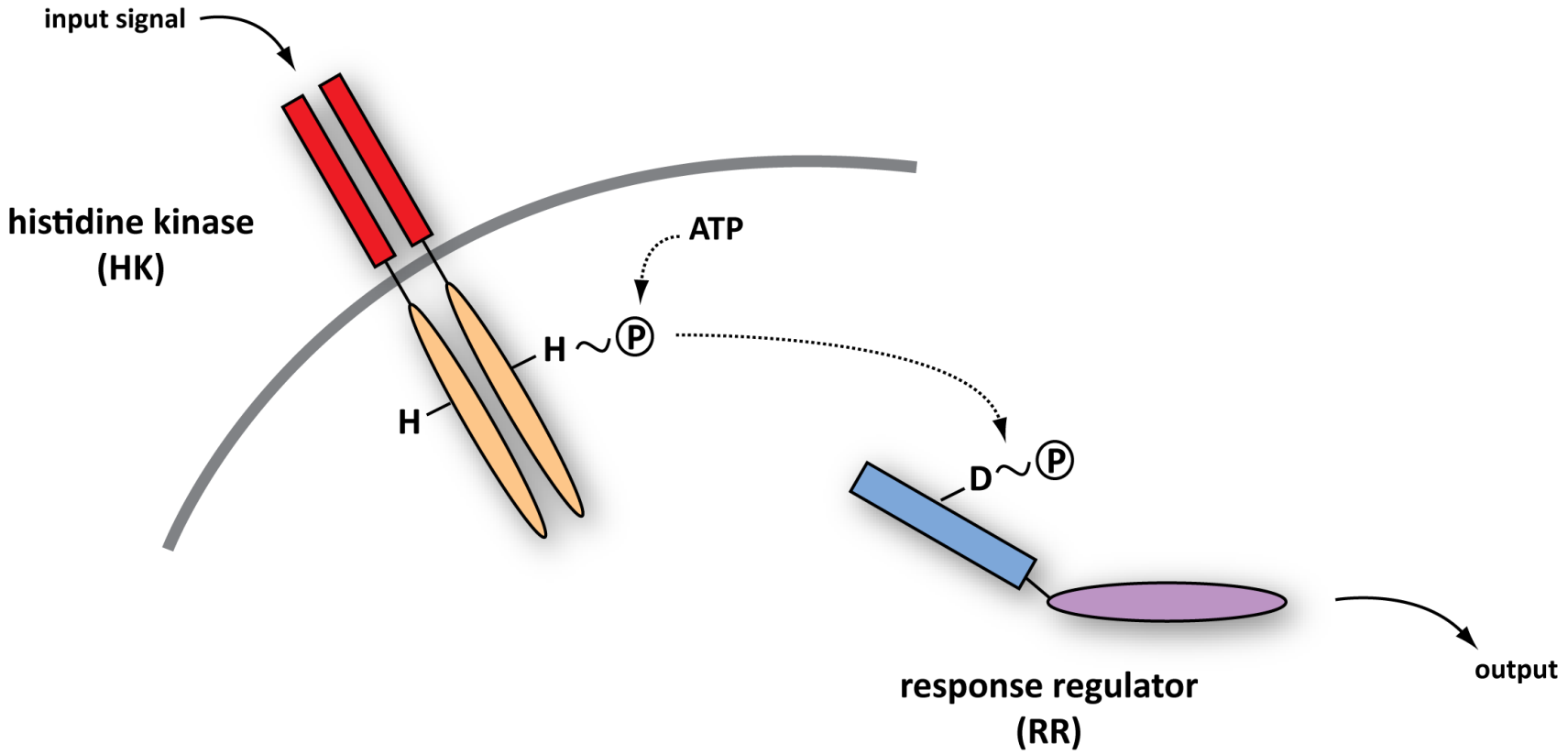

COORDINATING MULTIPLE SIGNALING SYSTEMS IN A SINGLE CELL

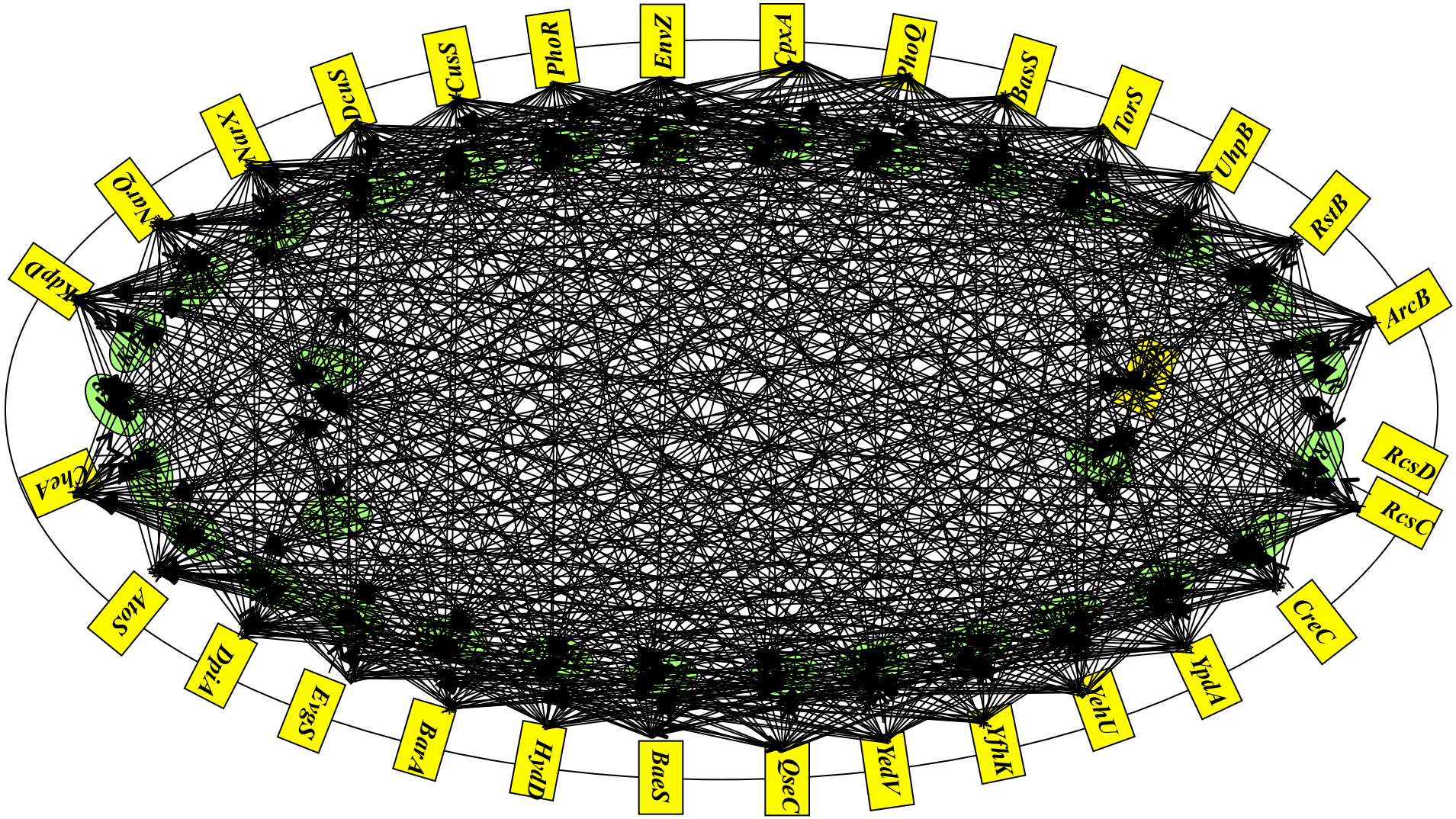

animation by Mark Gouilan

PHOSPHOTRANSFER PROFILING

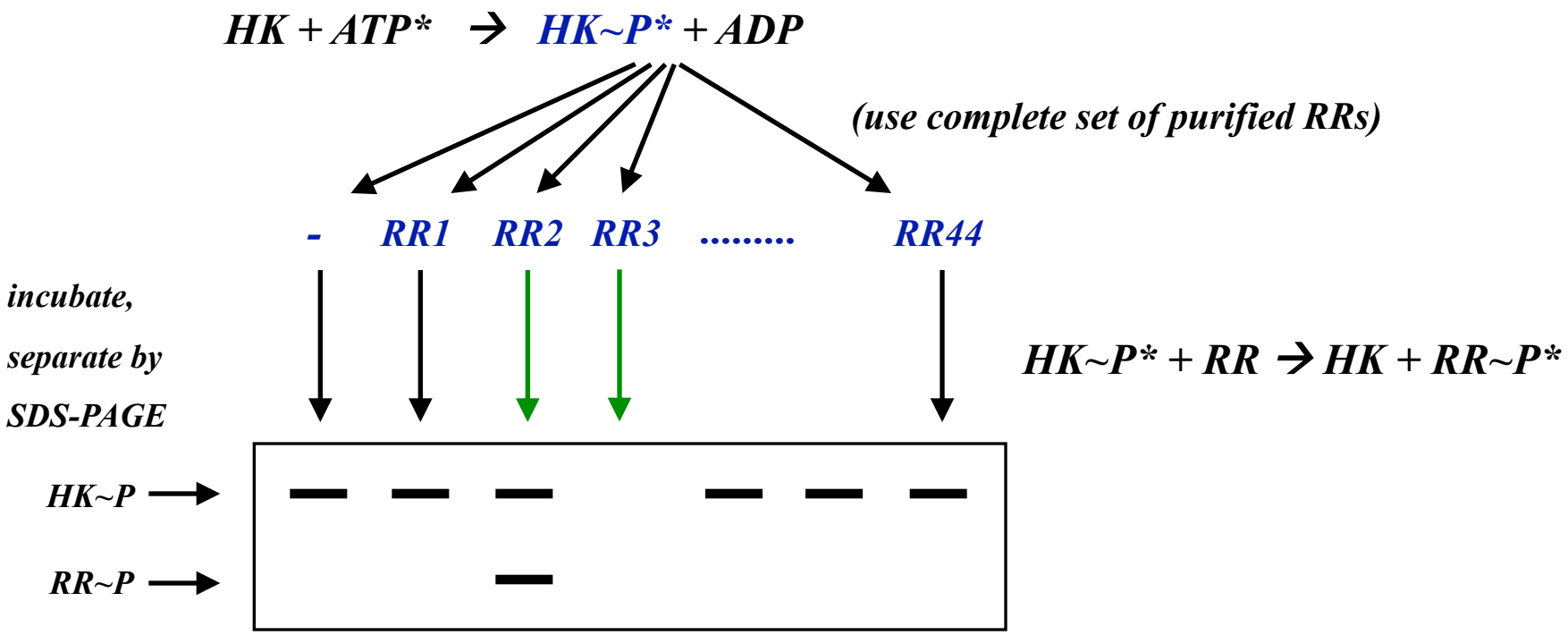

PHOSPHOTRANSFER PROFILING

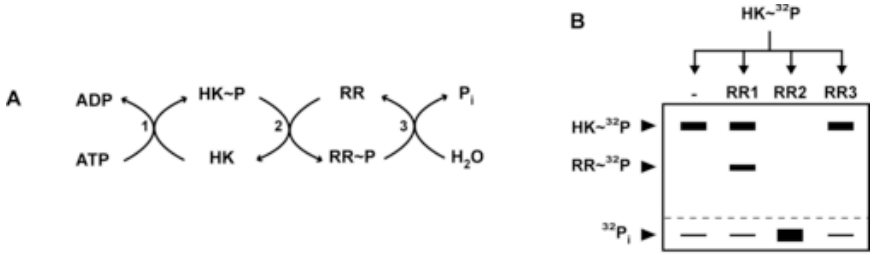

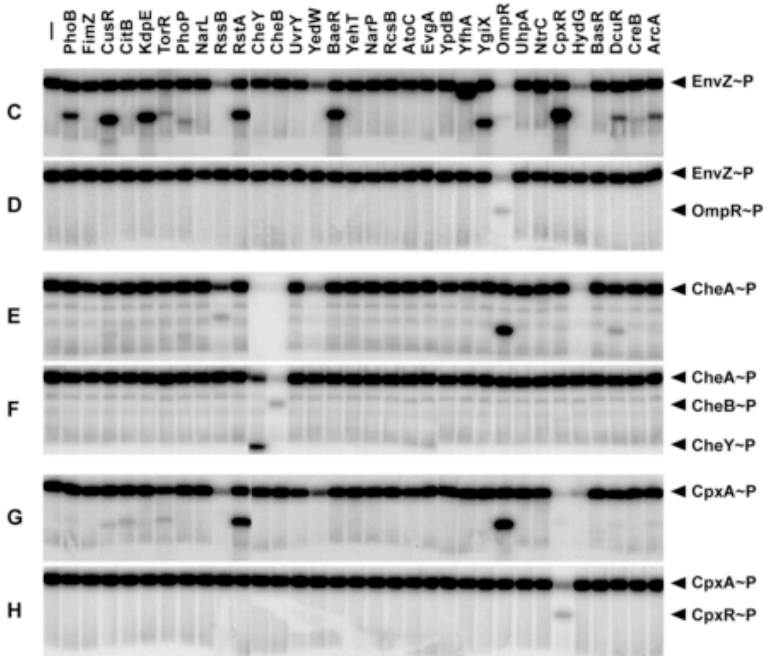

Figure 4. Phosphotransfer Profiling Method

(A) Phosphotransfer profile experiments involve three separate reactions: (1) autophosphorylation of the histidine kinase (HK) by radiolabeled ATP, (2) phosphotransfer to a response regulator (RR), and (3) dephosphorylation of the response regulator.

(B) Schematic of the phosphotransfer profiling technique. A single preparation of purified, autophosphorylated kinase (HK~^{32}P) is mixed with each response regulator from a given organism and analyzed for phosphotransfer by SDS-PAGE and autoradiography. The first lane shows a single band corresponding to the autophosphorylated histidine kinase and is used as a comparison for every other lane. Lanes 2–4 illustrate the three possible outcomes of a phosphotransfer reaction. In lane 2, phosphotransfer from HK to RR1 leads to the appearance of a band corresponding to RR1. In lane 3, phosphotransfer from HK to RR2 also occurs, but owing to high phosphatase activity (either autophosphatase or catalyzed by a bifunctional HK), the net result is production of inorganic phosphate (Pi) and the depletion of radiolabel from both the HK and RR2. In lane 4, no phosphotransfer occurs, and the lane is indistinguishable from lane 1.

(C–H) Phosphotransfer profiling was performed for three *E. coli* kinases (EnvZ, CheA, and CpxA) against all 32 purified *E. coli* response regulators, with phosphotransfer incubation times of either 1 h (C, E, and G) or 10 s (D, F, and H). For these three histidine kinases, a comparison of the short and long time point profiles indicates a kinetic preference for only their in vivo cognate regulators: OmpR (C and D), CheY and CheB (E and F), and CpxR (G and H). After being examined for phosphotransfer, all gels are stained with Coomassie to verify equal loading of histidine kinase and response regulator in each lane (data not shown). For each kinase profiled, we purified only its soluble, cytoplasmic domain, either as a thioredoxin-His_6 or a His_6-MBP fusion, using standard metal affinity chromatography (see Materials and Methods). When necessary, we made successive N-terminal truncations until we identified a construct that produced active kinase in vitro, always preserving the H-box and ATP binding domain (details on constructs used are in Table S3). All response regulators were purified as full-length fusions to a thioredoxin-His_6 tag. Purity was assessed by Coomassie staining, with each purified kinase domain and response regulator, except for *E. coli* FimZ, yielding an intense band of the correct approximate molecular weight (see Figure S5; Table S3).

DOI: 10.1371/journal.pbio.0030334.g004

(see Skerker, Laub et al..)

ASSESSING SPECIFICITY: PHOSPHOTRANSFER PROFILING

C. crescentus PhoR profile – 60 min phosphotransfer reactions

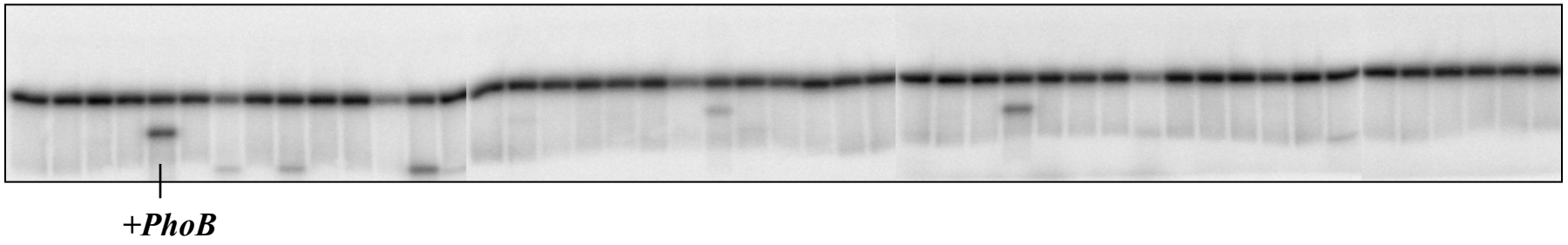

+PhoB

C. crescentus PhoR profile – 5 min phosphotransfer reactions

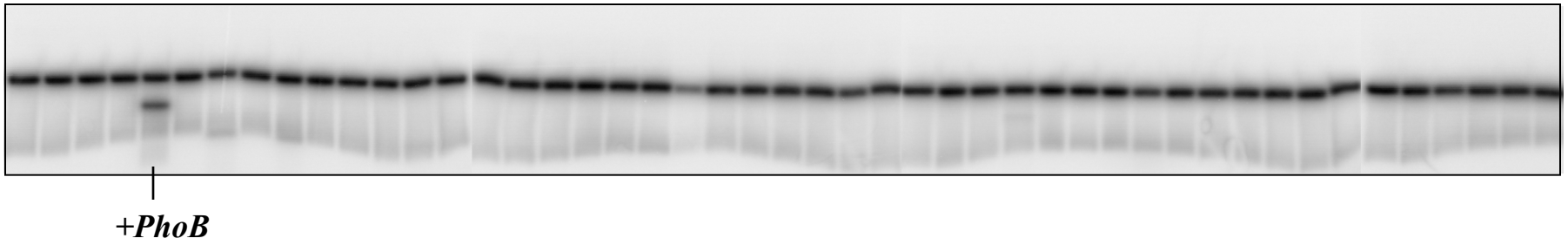

+PhoB

➔ ***histidine kinases exhibit a strong kinetic preference in vitro for their in vivo cognate substrate***

➔ ***specificity based on molecular recognition***

SIGNAL INTEGRATION

- Once we finish with our concrete example of chemotaxis, we will turn to the way in which cells decide where to put new actin filament and that will make us face this question of signal integration.
- Cell as a computer: not just amplification, but also logical operations such as AND, OR, etc.

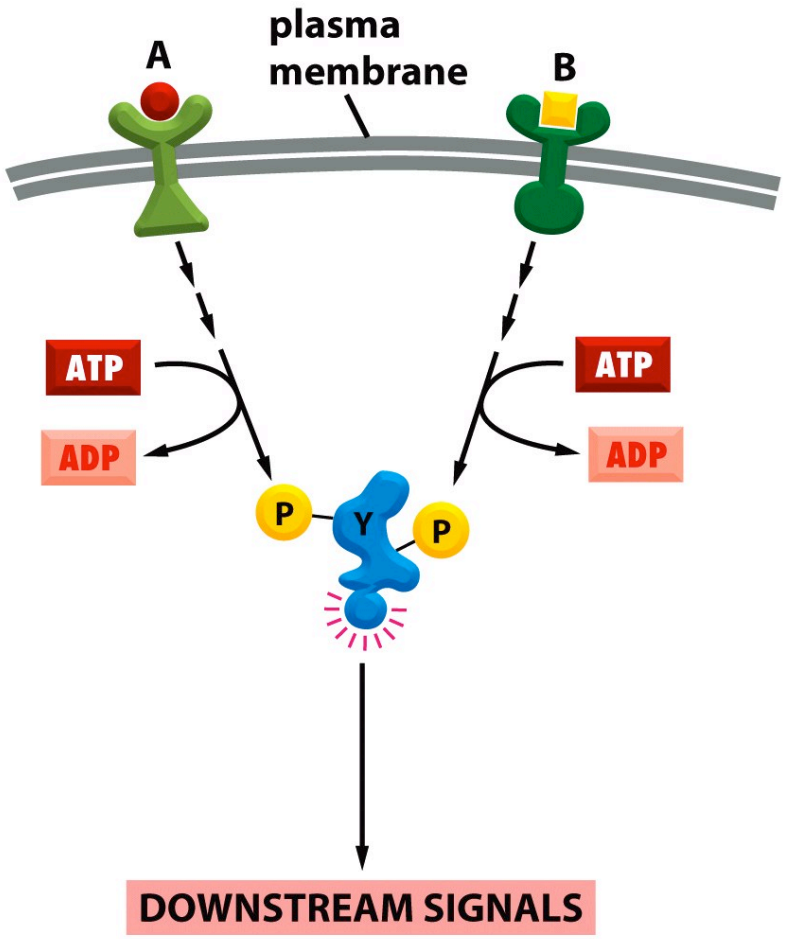

Figure 15-20 Molecular Biology of the Cell 5/e (© Garland Science 2008)

CELLULAR DECISIONS AND SWIMMING

- We have already seen the strategy of neutrophils for chasing down cellular offenders.
- Bacteria also exhibit motile strategies based upon environmental cues.

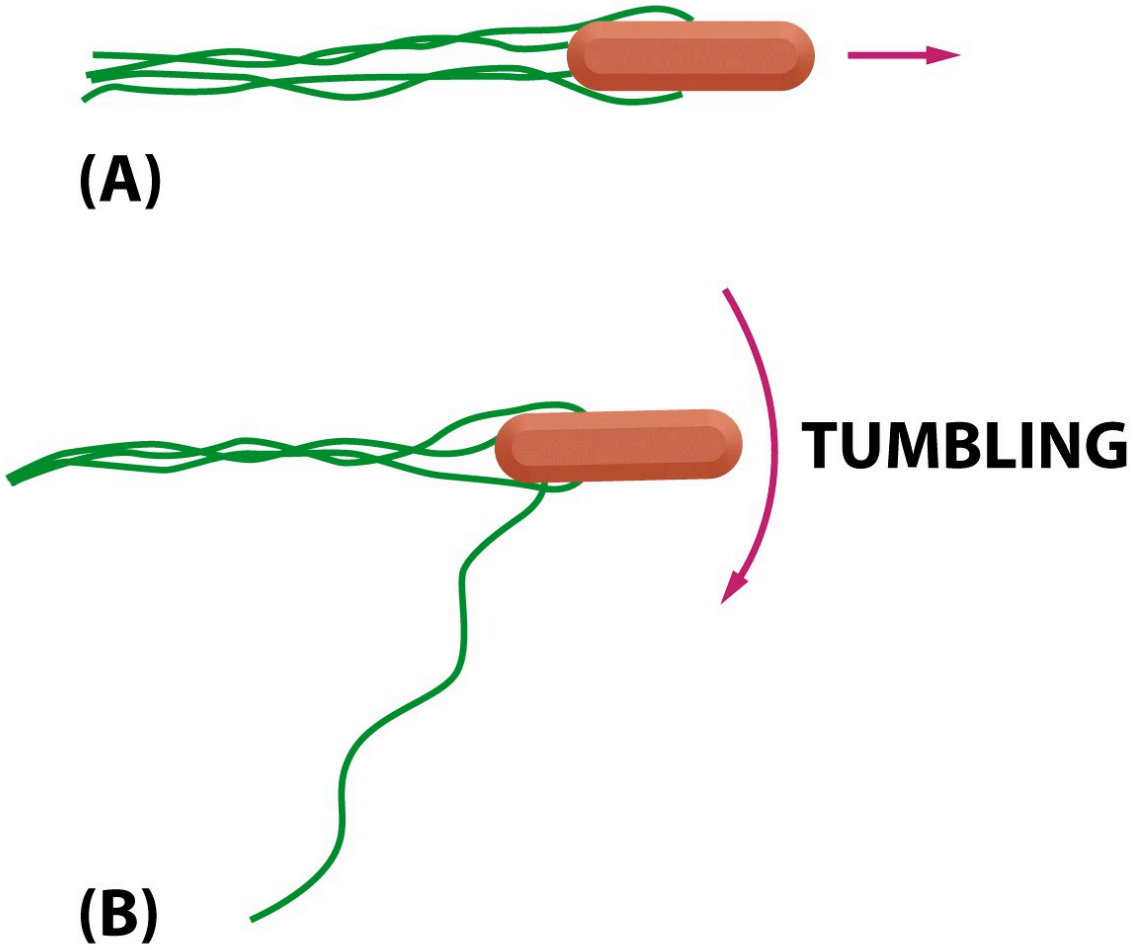

Figure 15-72 Molecular Biology of the Cell 5/e (© Garland Science 2008)

Cellular decisions and swimming

- We have already seen the strategy of neutrophils for chasing down cellular offenders.
- Bacteria also exhibit motile strategies based upon environmental cues.

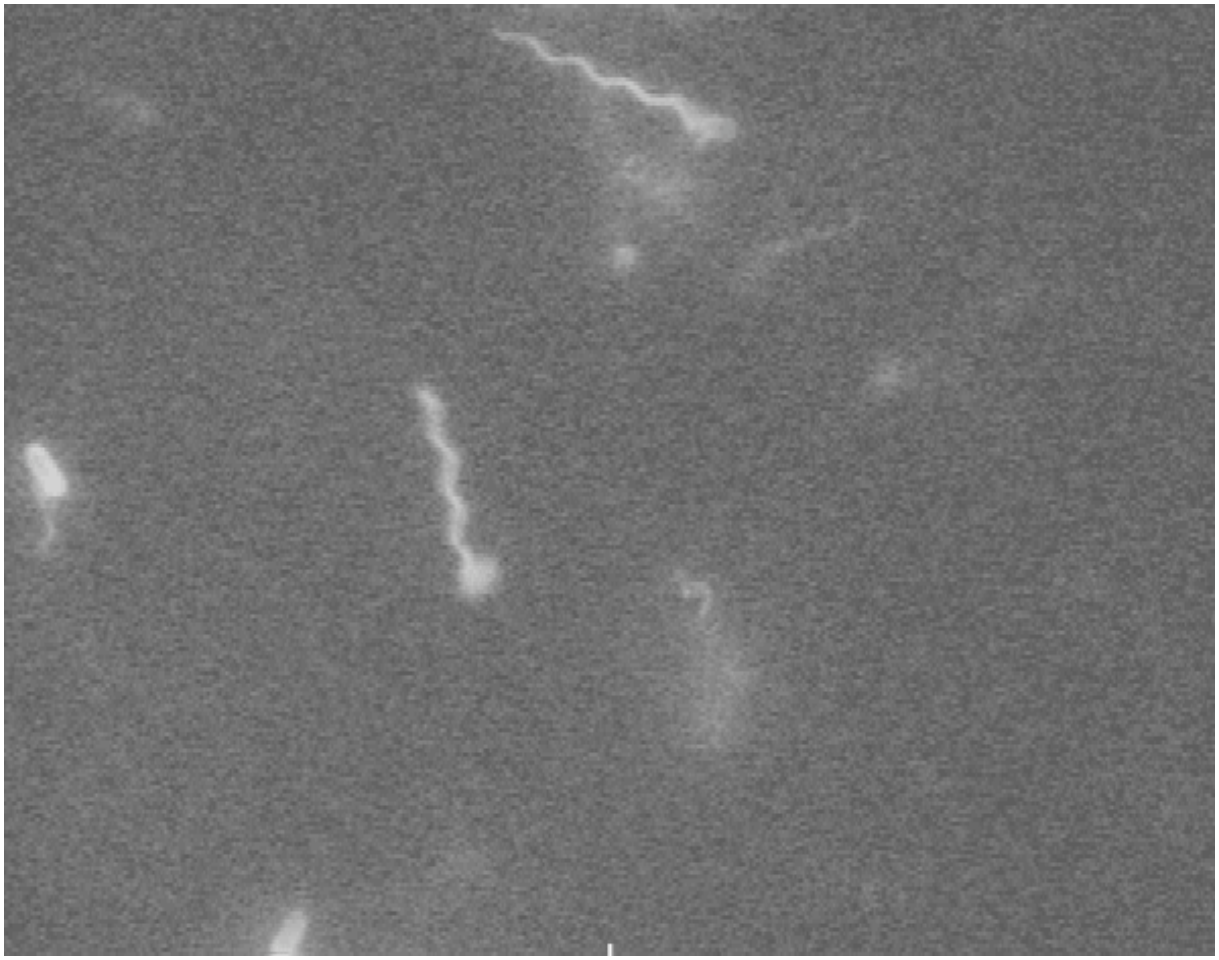

CELLULAR DECISIONS AND SWIMMING

- See the movies from Howard Berg website.

(see Turner, Ryu, Berg – J. Bacteriol. 2000 .)

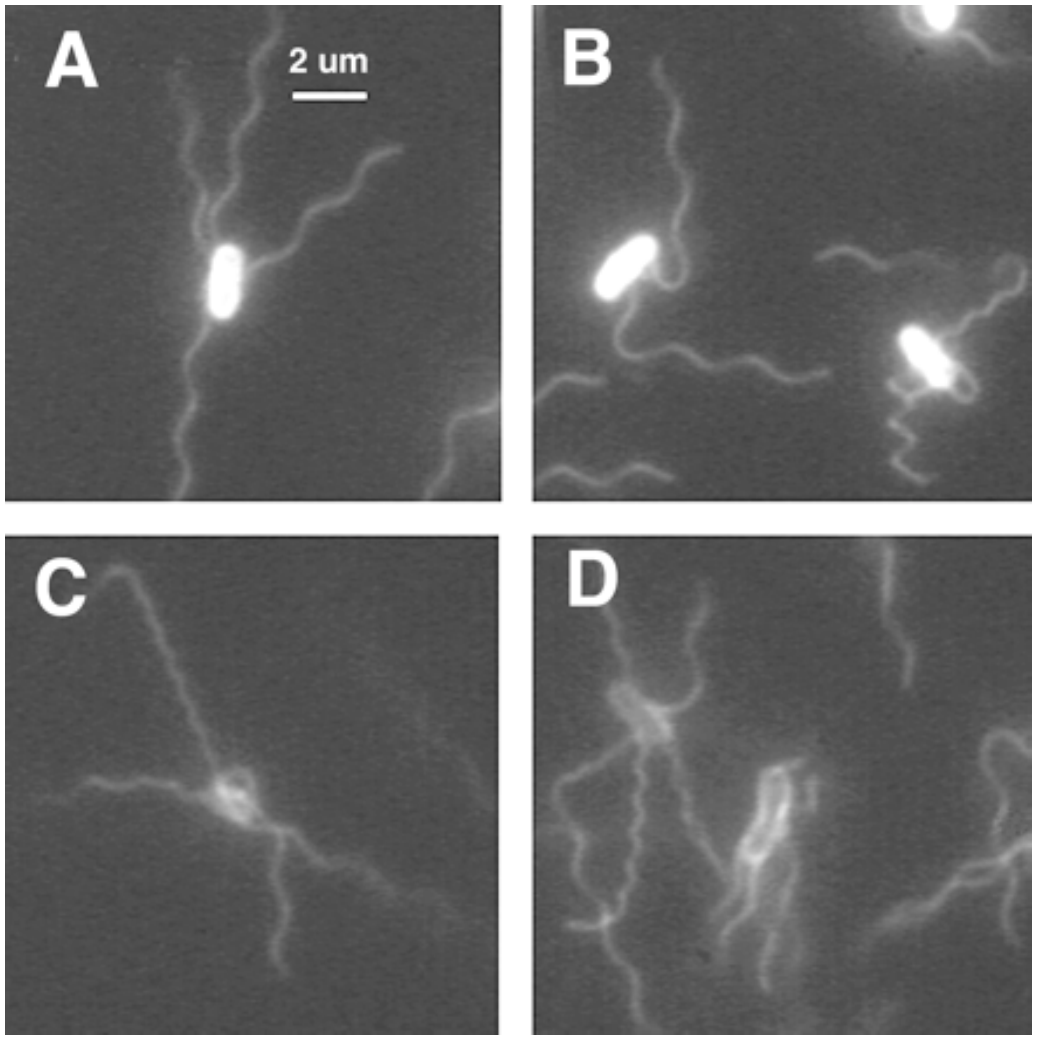

A GENERAL VIEW OF BACTERIAL CHEMOTAXIS

- We will return to this figure several times in order to clarify various aspects of the bacterial chemotactic response.

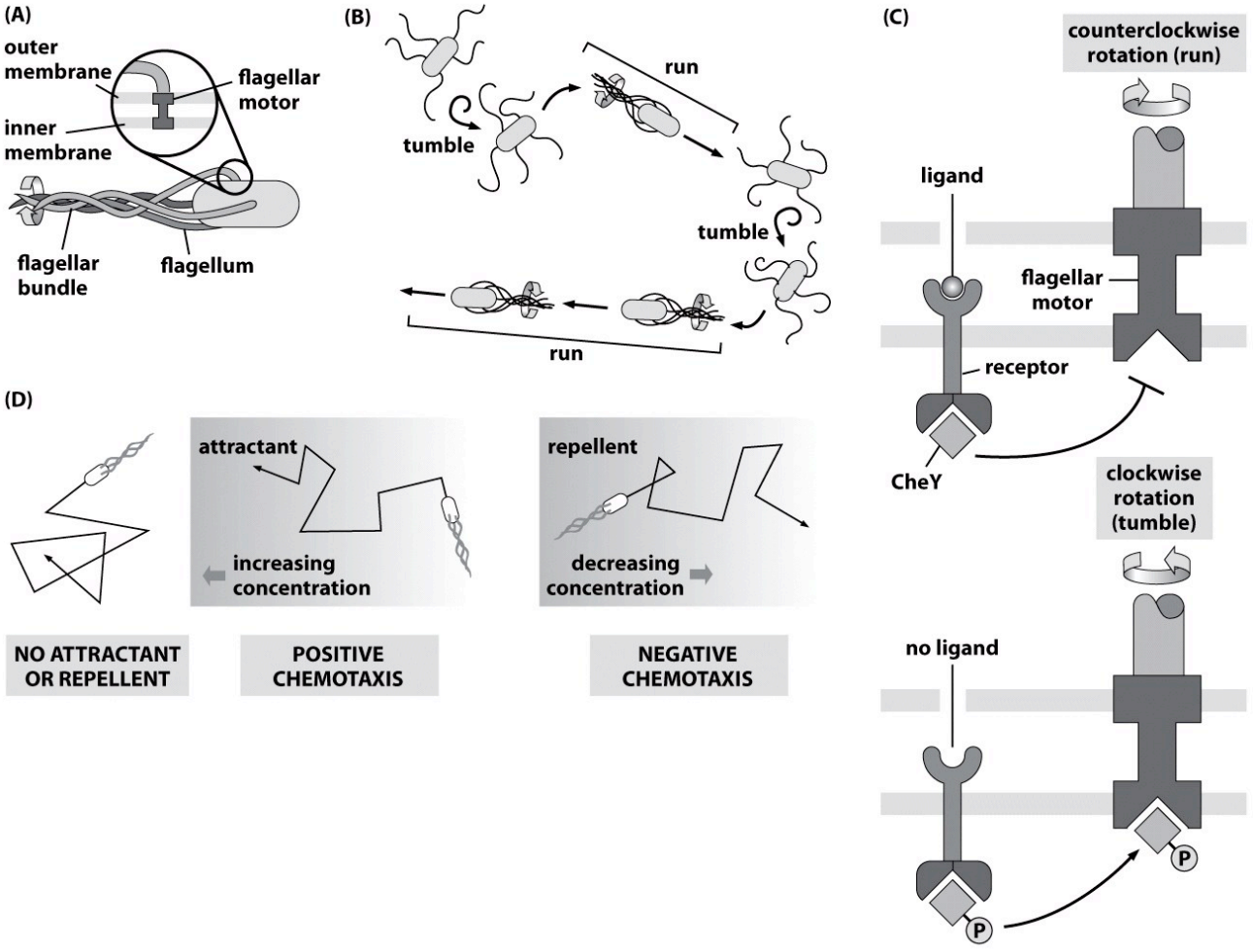

Figure 4.16 Physical Biology of the Cell (© Garland Science 2009)

AN AMAZING MOLECULAR MACHINE

- The flagellar motor uses a proton gradient to rotate at roughly the angular speed of a jet engine.
- This motor is a darling of the creationists as an example of something that "couldn't have evolved" because of its supposed "irreducible complexity".

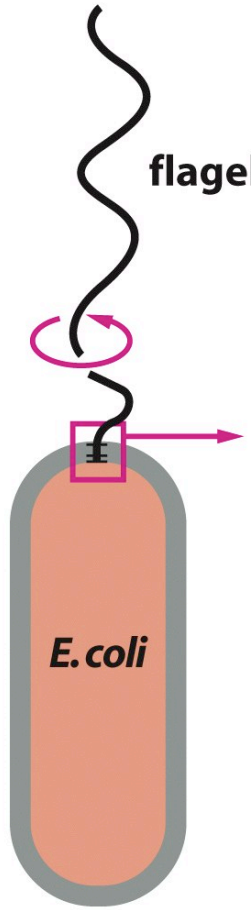

Figure 15-71a part 1 of 2 Molecular Biology of the Cell 5/e (© Garland Science 2008)

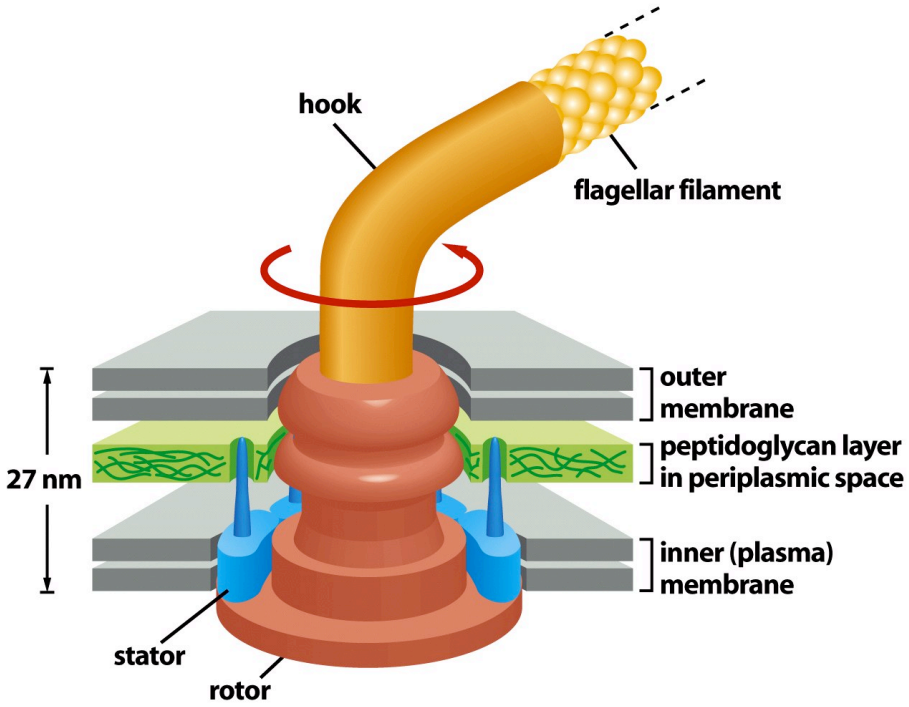

Figure 15-71a part 2 of 2 Molecular Biology of the Cell 5/e (© Garland Science 2008)

BACTERIAL CHEMOTAXIS CIRCUIT

- The circuit for bacterial chemotaxis involves precisely the kind of two-component signal transduction system that we discussed earlier.

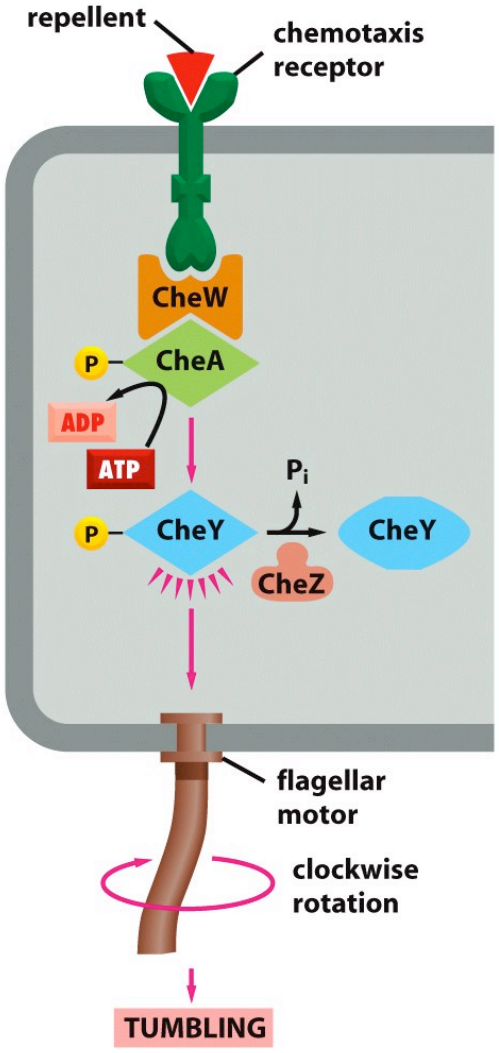

Figure 15-73 Molecular Biology of the Cell 5/e (© Garland Science 2008)

CELLULAR DECISIONS AND SWIMMING

- Concept of experiment: tether cell to surface and watch the rotation of the motor. They use a second color to watch the CheY-P in the cell. The result is a plot that shows the frequency of motor tumble rate as a function of CheY-P.

(see Cluzel, Surrette and Leibler, Science.)

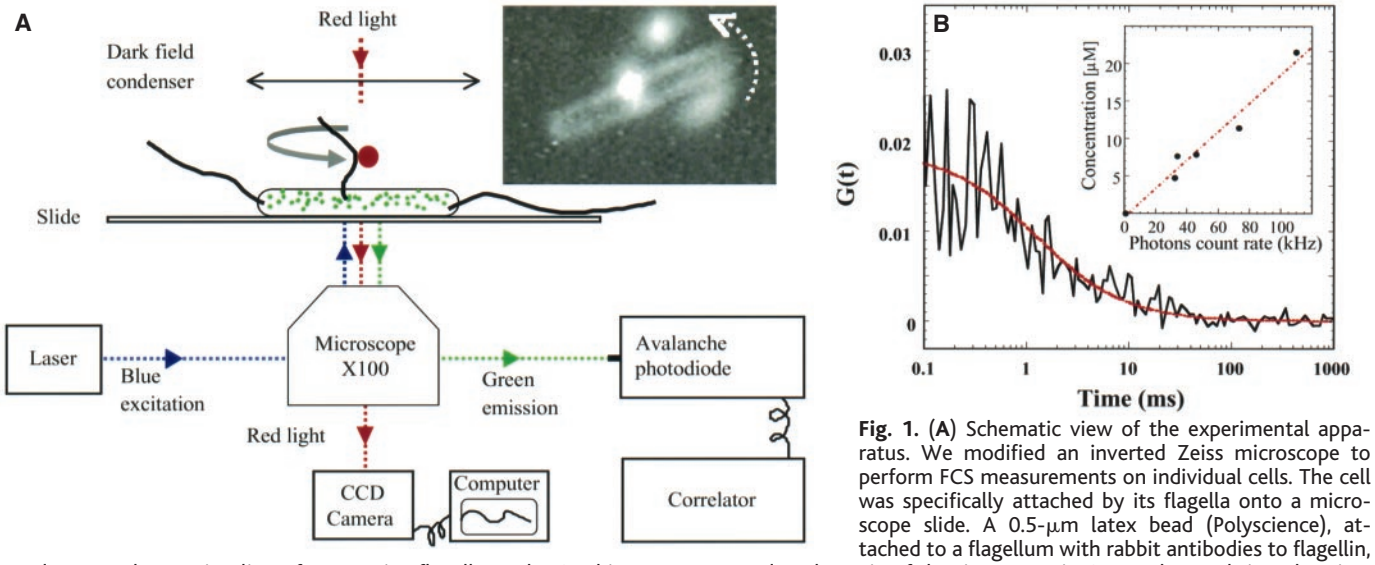

Fig. 1. (**A**) Schematic view of the experimental apparatus. We modified an inverted Zeiss microscope to perform FCS measurements on individual cells. The cell was specifically attached by its flagella onto a microscope slide. A 0.5-μm latex bead (Polyscience), attached to a flagellum with rabbit antibodies to flagellin, is used as a marker to visualize a free rotating flagellum. The CW bias was computed as the ratio of the time spent in CW to the total time duration. The FCS technique allowed us to measure GFP-tagged protein concentration in the same bacterium. The fluctuations of the total fluorescence intensity were processed in real time by a correlator (ALV-5000/E) that provided an autocorrelation function (*14*). CCD, charge-coupled device. (**Inset**) A dark-field illumination (red light) was used to record the rotation of a single flagellum of a bacterium attached to a cover slip. For clarity, only three images, 1/15 s apart, were superimposed to show the circular trajectory of the bead. [When a bead was attached to several flagella, its trajectory was no longer circular and it moved erratically. Here, the bead was rotating CCW, a state corresponding to smooth swimming (*9*)]. (**B**) Typical autocorrelation function measured for diffusing CheY-P–GFP molecules in a single cell. The amplitude of the autocorrelation function at the intercept with the vertical axis is inversely equal to the number of molecules (N) in the detection volume. We fit this function (continuous red line) with $G(t) = 1/N[1 + (4Dt/\omega^2)]^{-1}$, which describes two-dimensional translational diffusion (*15*). D is the diffusion constant of the fluorescent molecules, t is the time variable, and $2\omega = 0.3$ μm is the diameter of the detection volume in our experimental configuration; one molecule in this volume represented a concentration of 44 nM. The autocorrelation functions were measured from acquisitions of 7 s. The average diffusion constant of the cytoplasmic CheY-GFP fusion, evaluated from this fit, was 4.6 ± 0.8 μm^2 s^{-1} (*16*). (**Inset**) A typical calibration curve, providing a linear relation between concentration of CheY-P–GFP and the fluorescent light intensity for five individual cells. Protein concentrations on this curve were obtained with the FCS technique. We then used the calibration curve to convert fluorescence intensity into GFP concentration in those cells whose flagellar rotation was monitored. This method reduced the photobleaching of GFP by measuring the fluorescence intensity for only 0.5 s (*17*).

CELLULAR DECISIONS AND SWIMMING

- Measure the response of the motor as a function of the concentration of CheY-P.
- Clockwise bias (CW) is obtained by taking fraction of time spent in clockwise state divided by the total time.

(see Cluzel, Surrette and Leibler, Science.)

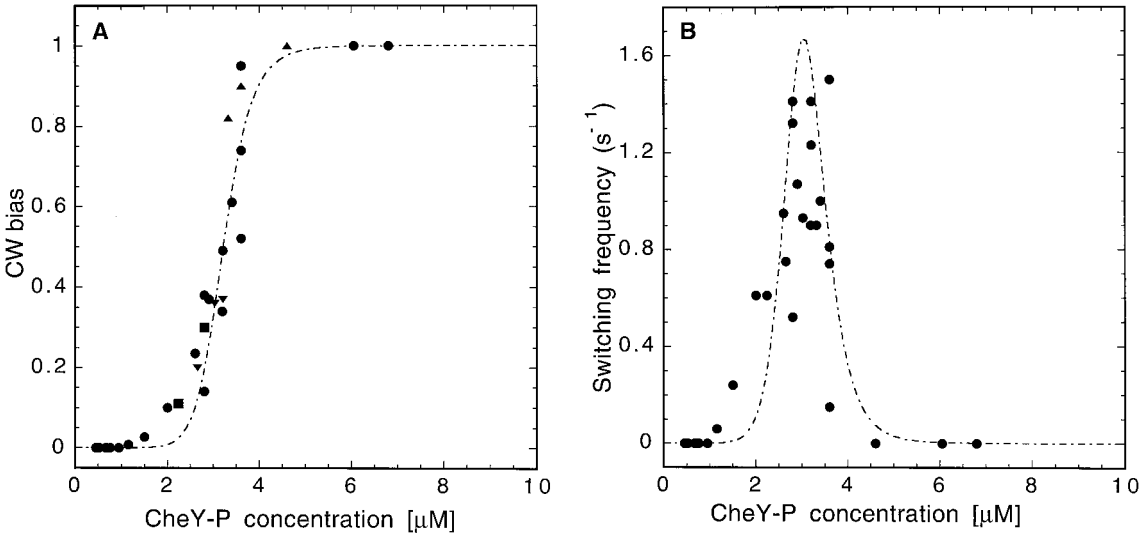

Fig. 2. (**A**) Characteristic response of individual motors as a function of CheY-P concentration. Each data point describes a simultaneous measurement of the motor bias and the CheY-P concentration in an individual bacterium. The CW bias was computed by analyzing video recordings for at least 1 min. We introduced the *cheY-gfp* (*13*) fusion gene into the strain PS2001. It is believed that in this strain, all CheY molecules are phosphorylated (*12*). Cells were grown from an overnight culture in tryptone broth at 30°C and then harvested (absorbance = 0.5 at 595 nm). To cover the whole range of motor response, we grew cells with three different IPTG concentrations (0, 5, and 10 μM) and then washed and resuspended them in minimum medium ●. The second set of experiments was also performed to check whether the folding kinetics of the GFP would affect the CheY-P activity under our experimental conditions. The expression of CheY-P–GFP fusion was monitored after the Luria-Bertoni (LB) medium was saturated with 10 mM IPTG. While the cells were expressing the CheY-P–GFP fusion, the motors' bias would increase and follow the same sigmoid curve (*21*). Time points correspond to 18, 28, and 33 min for ▼, to 60 and 69 min for ■, and to 17, 23, and 26 min for ▲, after the IPTG was added. The dashed line shows the best fit obtained with a Hill function (Hill coefficient $N_H = 10.3 \pm 1.1$ and $K_M = 3.1$ μM). Motors were locked in (CW) state for tested CheY-P concentrations ranging from ~4.6 to 25 μM (*27*). (**B**) Switching frequency, *F*, measured from the same cells as in (A). *F* was defined as the number of times that a motor switched its direction of rotation divided by the duration of the recording. In agreement with previous observations, we observe that the data points for the switching frequency are more scattered than those obtained for the motor bias (*5*). The dashed line gives the first derivative of the Hill function [from (A)] with respect to [CheY-P]. It is interesting to note that *F* qualitatively behaves as $F \sim [\partial(\text{CW-bias})/\partial C]$, where *C* is [CheY-P].

THE FRET TECHNIQUE

- Fluorescence resonance energy transfer is an amazing molecular ruler.
- Proximity of acceptor and donor is readout by the efficiency of the transfer.

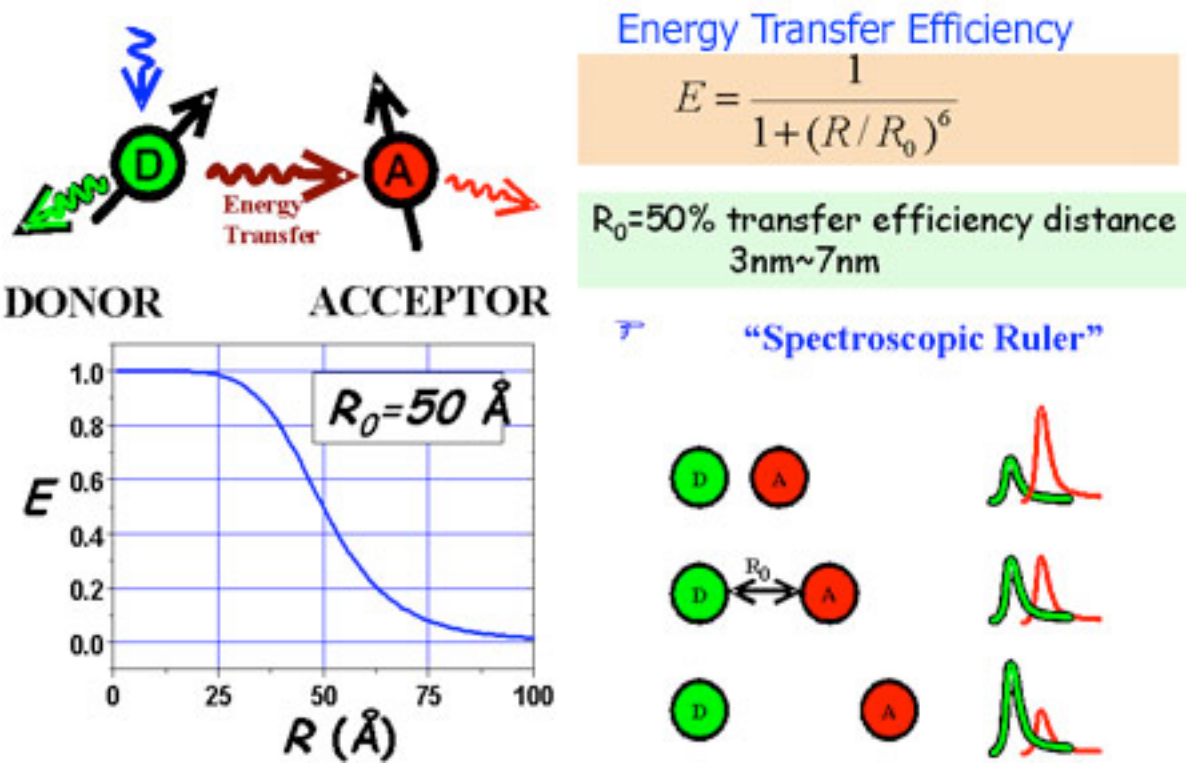

https://netfiles.uiuc.edu/tjha/www/images/FRET_concept.jpg

FRET AND CHEMOTAXIS

- FRET between CheY-P and CheZ.
- This is from the paper of Sourjik and Berg, PNAS, 2002. They have two papers in PNAS that year, this is the first one.

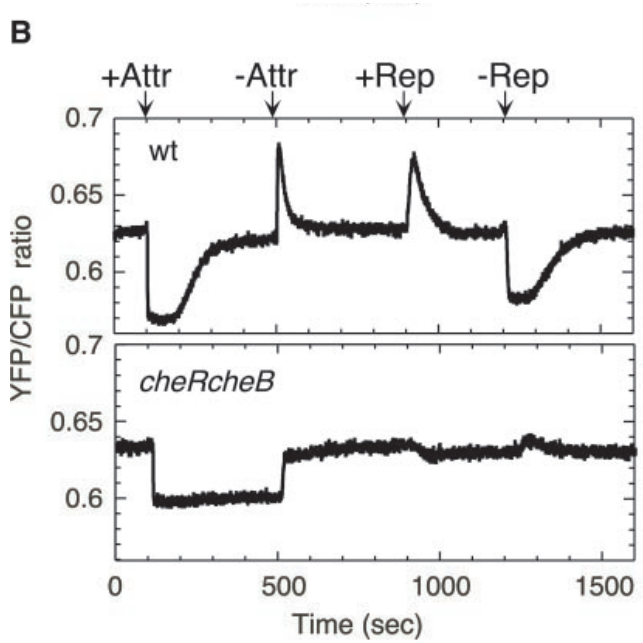

Fig. 1. Changes in protein–protein interactions observed by FRET upon chemotactic stimulation of cells of *E. coli* adsorbed to a coverslip. (*A*) Experimental scenario. Cells containing CheY/CheZ pairs were stimulated by stepwise addition or removal of attractant, MeAsp, as indicated by the dashed line (simulated by the flow of 0.5 μM fluorescein). Changes in protein–protein interactions result in changes in the ratio of fluorescence intensities of YFP and CFP. ΔR_{init} is the initial response to addition or removal of attractant. (*B*) FRET responses to addition/removal of attractant and to addition/removal of repellent for wild-type (wt) and mutant cells (*cheRcheB*) defective for methylation/demethylation. Stimulation levels were chosen to cause a near-saturating response. Attractant (Attr): 30 μM MeAsp for wt, 1.5 mM for *cheRcheB*. Repellent (Rep): 100 μM $NiCl_2$.

CHANGES IN INTERACTIONS BETWEEN LABELED PROTEINS OBSERVED BY FRET ON CHEMOTACTIC STIMULATION OF E. COLI CELLS

- The circuit for bacterial chemotaxis involves precisely the kind of two-component signal transduction system that we discussed earlier.

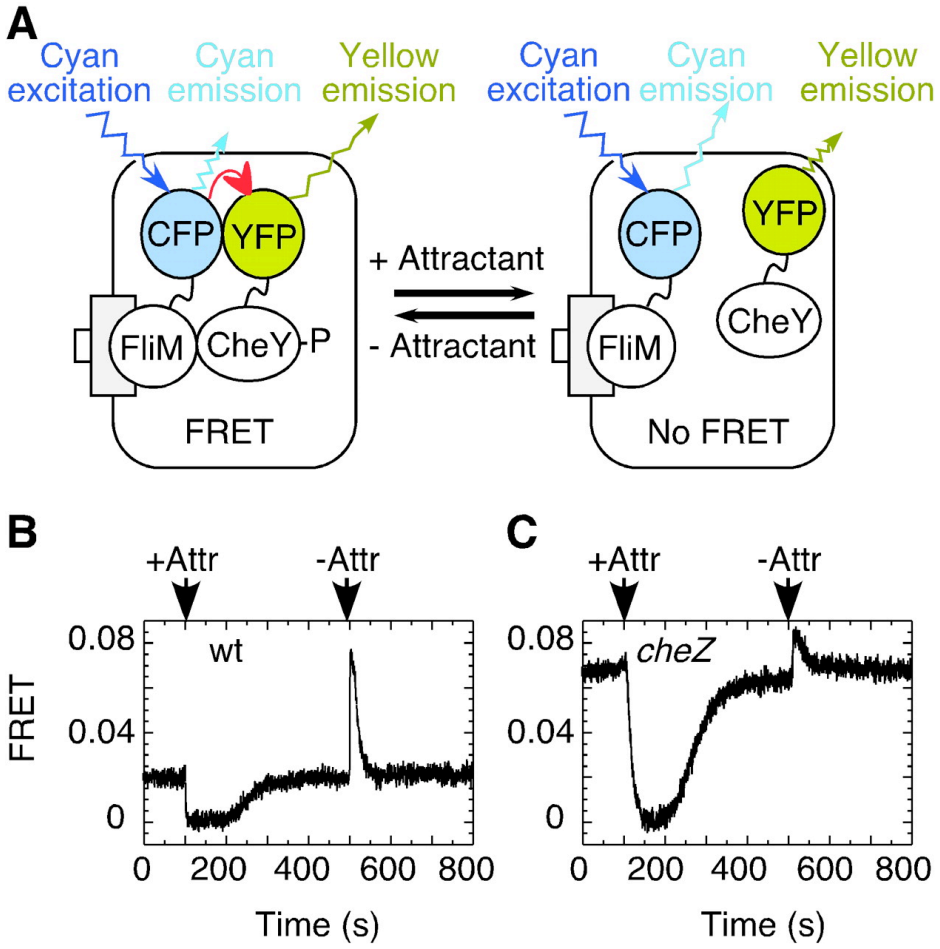

Sourjik V, Berg H C PNAS 2002;99:12669-12674

Receptor Activity and Chemoattractant Concentration

- Measure the FRET activity for different chemoattractant concentrations.
- Different mutants have different adaptive responses.

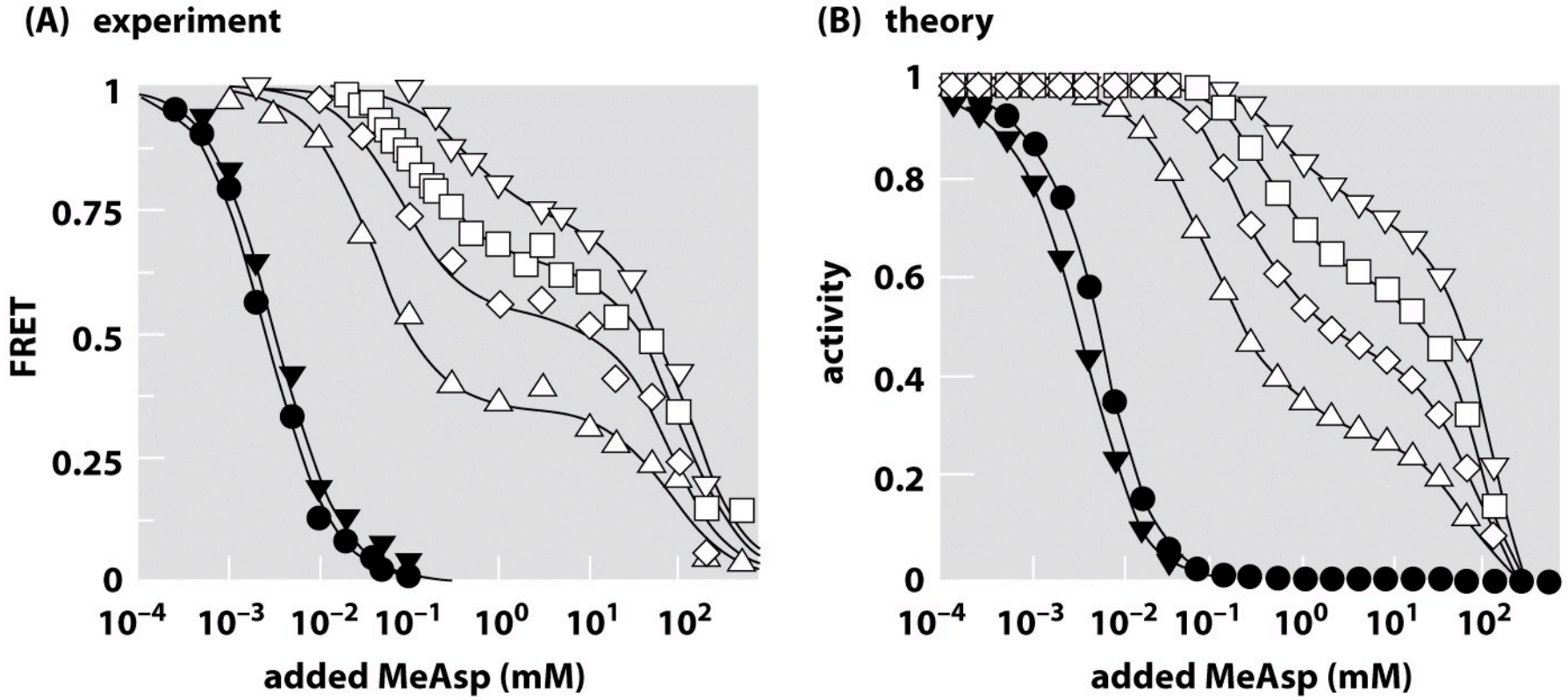

Figure 19.34 Physical Biology of the Cell (© Garland Science 2009)

Motor binding and bias

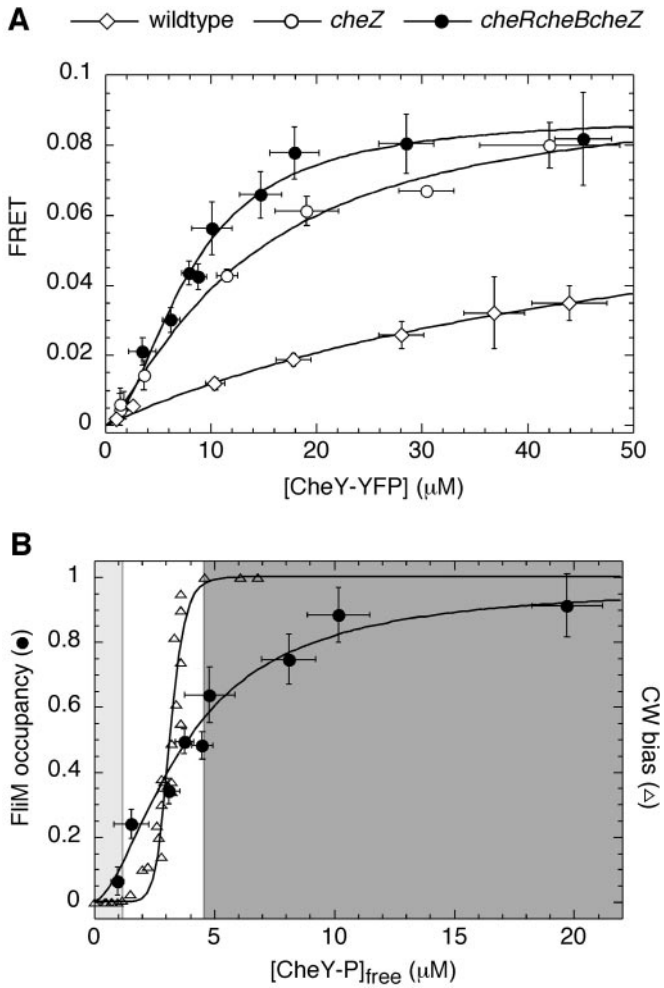

Fig. 2. Binding curves for CheY-YFP/CFP-FliM measured *in vivo*. (*A*) Dependence of FRET signals from unstimulated cell populations of wild-type (◇), *cheZ* (○), and *cheRcheBcheZ* (●) cells on the expression level of CheY-YFP, varied by induction with IPTG (0–0.3 mM). The CheY-YFP and CFP-FliM concentrations were determined as described in *Materials and Methods*. (*B*) Comparison of dependence of motor bias (△) and FliM occupancy (●) on concentration of free cytoplasmic CheY~P, $[\text{CheY}\sim\text{P}]_{\text{free}}$. Data for the motor bias and parameters for the Hill fit (dashed curve, $H = 10.3$, $K_{1/2} = 3.1$ μM) are taken from ref. 8. Data for FliM occupancy are recalculated from the data for the *cheR cheB cheZ* cells in (*A*) assuming that a FRET value of 0.088 corresponds to a FliM occupancy of 1, as explained in the text. Only part of the data are shown. The light-shaded area (*Left*) indicates the range of CheY~P concentrations over which the rotation of the motor is exclusively counterclockwise, the unshaded area (*Center*) the range of concentrations over which the motor switches, and the dark-shaded area (*Right*) the range of concentrations over which the rotation is exclusively clockwise (CW). Fits by the Hill model are shown by solid lines. Error bars represent standard deviations of multiple experiments.

BUILDING A STATISTICAL MECHANICS MODEL

- Our goal is to find the probability that the receptor will be in the on state as a function of the chemoattractant concentration.

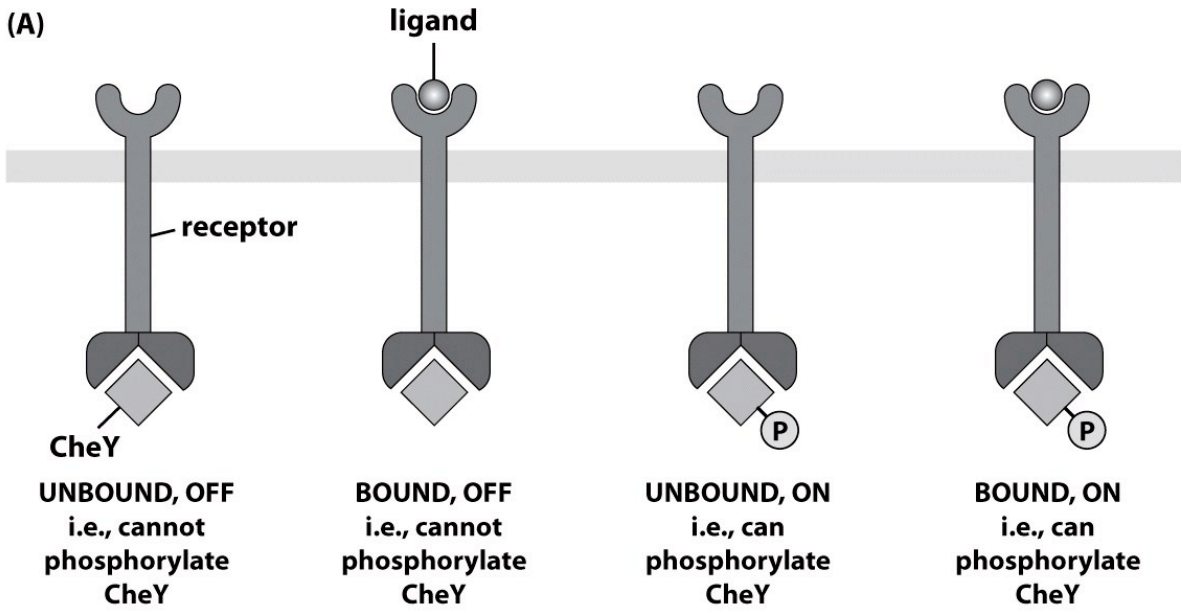

Figure 19.32 Physical Biology of the Cell (© Garland Science 2009)

STATES AND WEIGHTS

- Each of the states has a corresponding statistical weight.

STATE	WEIGHT
	$\frac{\Omega!}{L!(\Omega-L)!}\, e^{-\beta L \varepsilon_{sol}}\, e^{-\beta \varepsilon_{off}}$
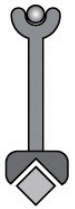	$\frac{\Omega!}{(L-1)!(\Omega-(L-1))!}\, e^{-\beta (L-1) \varepsilon_{sol}}\, e^{-\beta \varepsilon_{off}}\, e^{-\beta \varepsilon_b^{off}}$
	$\frac{\Omega!}{L!(\Omega-L)!}\, e^{-\beta L \varepsilon_{sol}}\, e^{-\beta \varepsilon_{on}}$
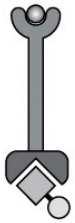	$\frac{\Omega!}{(L-1)!(\Omega-(L-1))!}\, e^{-\beta (L-1) \varepsilon_{sol}}\, e^{-\beta \varepsilon_{on}}\, e^{-\beta \varepsilon_b^{on}}$

Figure 19.33 Physical Biology of the Cell (© Garland Science 2009)

CHANGES IN FLIM OCCUPANCY AFTER FLASH-RELEASE OF CAGED CHEMOEFFECTORS

- After addition of a chemoattractant, the FRET measurements permit direct determination of the kinetics of the process.

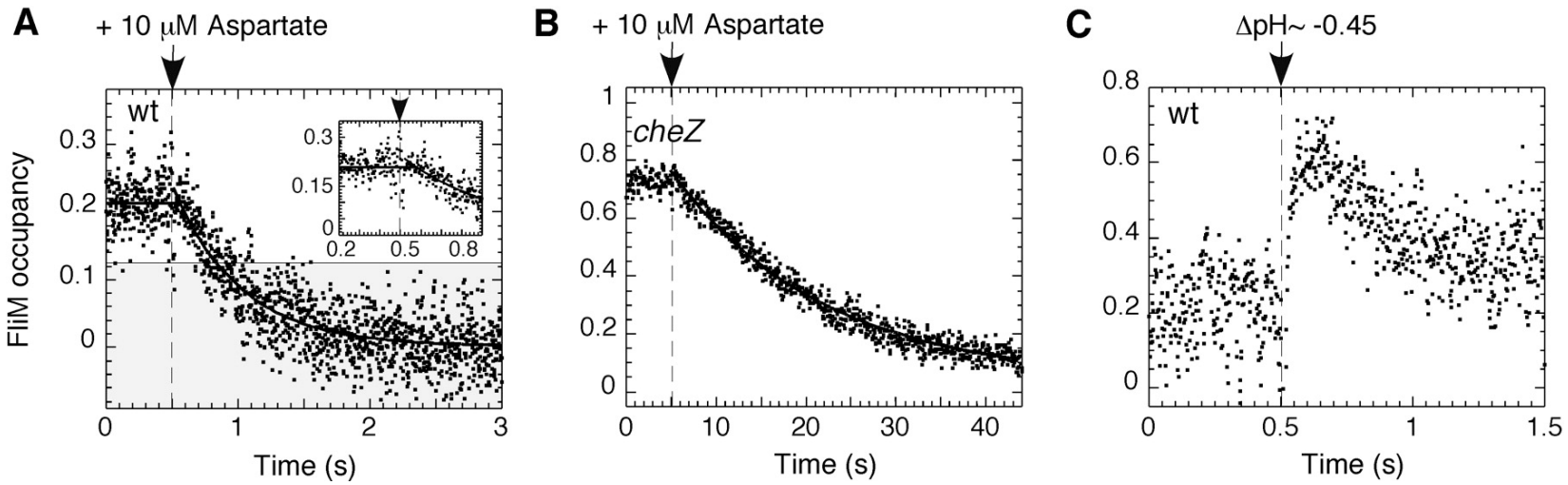

Sourjik V, Berg H C PNAS 2002;99:12669-12674

ADAPTATION OF THE CIRCUIT

- Methylation provides a scheme for tuning the energy difference between the on and off states of the receptor complex.
- Quantitative measurements leave us with many interesting questions: mutants and their responses, sharpness of response, adaptation, motor binding vs switching, etc…

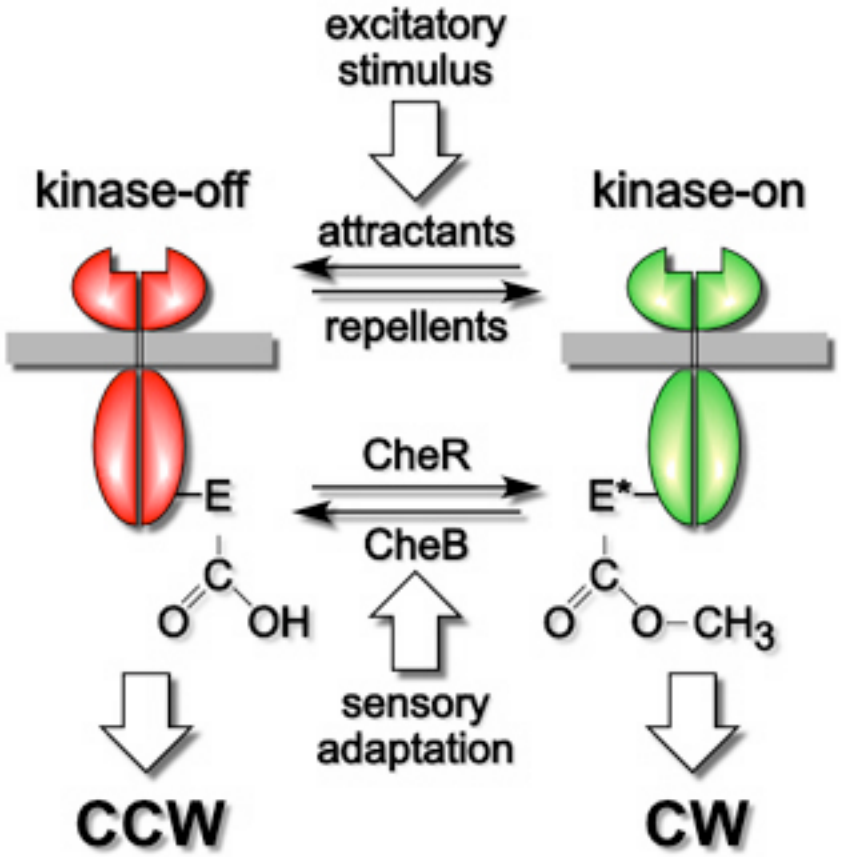

Parkinson lab - Utah

High Resolution Imaging of Chemotaxis Proteins

- PALM is a high-resolution technique that permits beating the diffraction limit.
- In this case, they are looking at chemotaxis proteins in *E. coli*.

(Greenfield, Liphardt et al, PLoS Biology, 2009.)

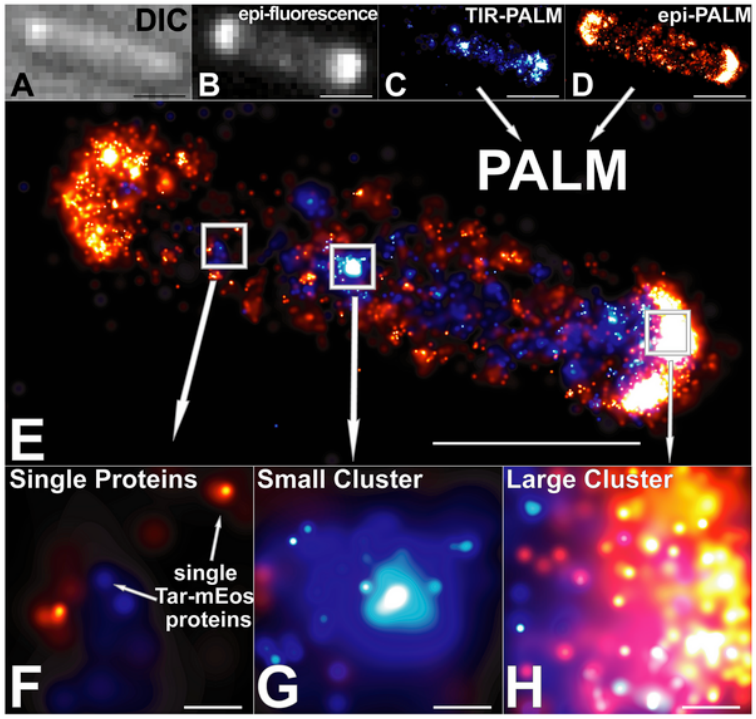

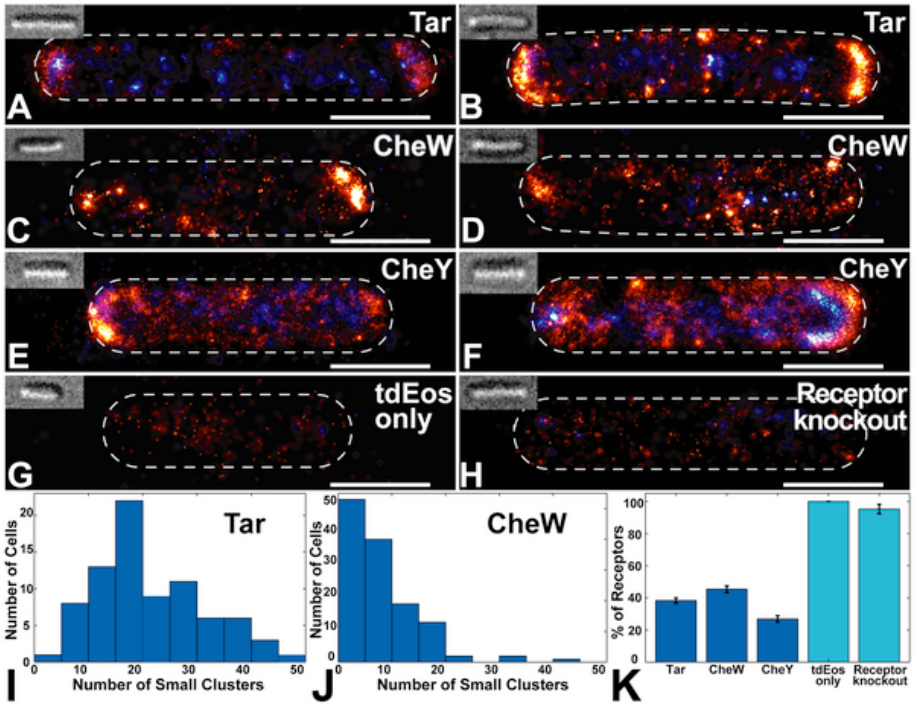

NATURE OF THE RECEPTORS

- Receptors assemble into trimers of dimers.
- Receptor clustering is part of the overall story.

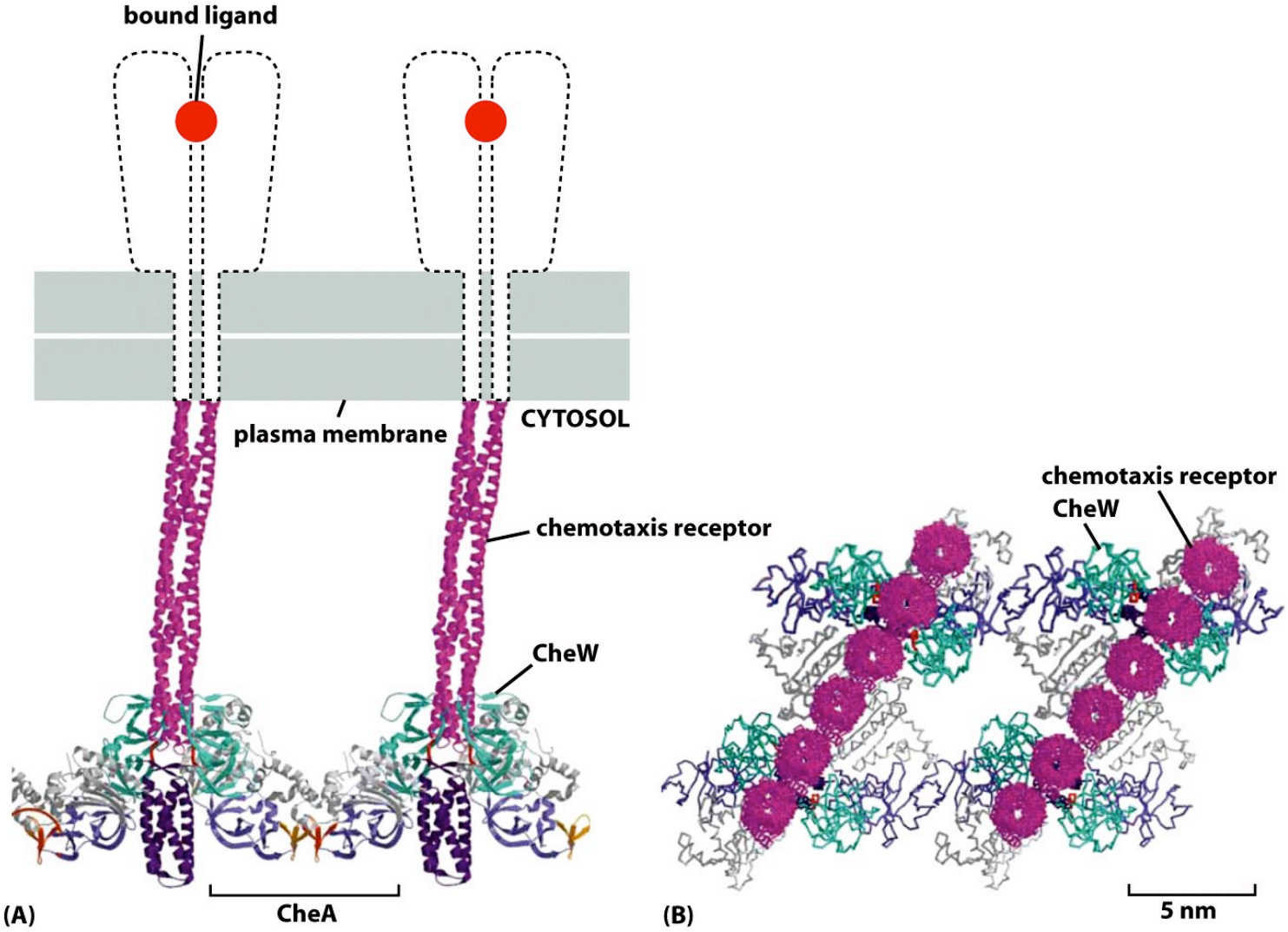

Figure 15-74 Molecular Biology of the Cell 5/e (© Garland Science 2008)

CELLS DECIDE: WHERE TO GO

The Hunters of the Immune Response

- ***There is another kind of rapid response to environmental cues that is much faster than gene regulation.***
- ***The "decision" about where to go next is highly regulated and results in the synthesis of new cytoskeletal filaments at the leading edge of the cell.***
- ***Once again, there is an interesting random walk story behind the scenes.***

Cell Motility and Actin Polymerization

- ***Motility is driven by the protein actin. Actin assembles into long filaments.***
- ***Through hydrolysis of ATP, these filaments can actually do work as a result of this polymerization process by pushing on membranes, for example.***

(Theriot et al.)

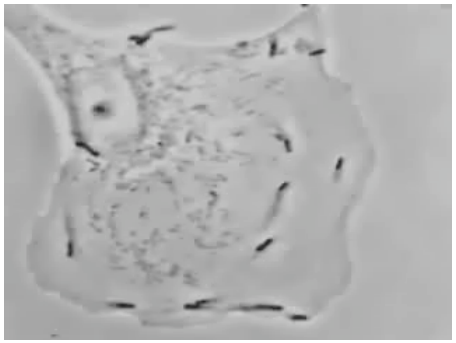

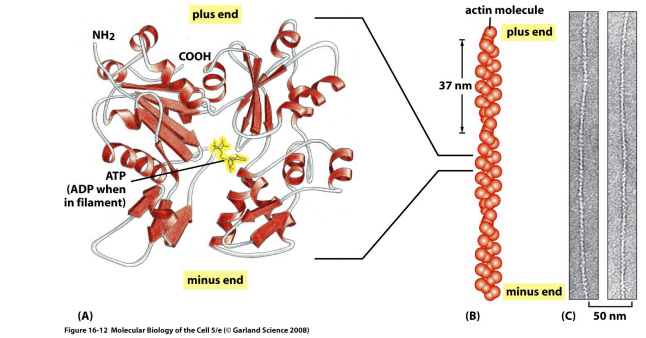

Figure 16-12 Molecular Biology of the Cell 5/e (© Garland Science 2008)

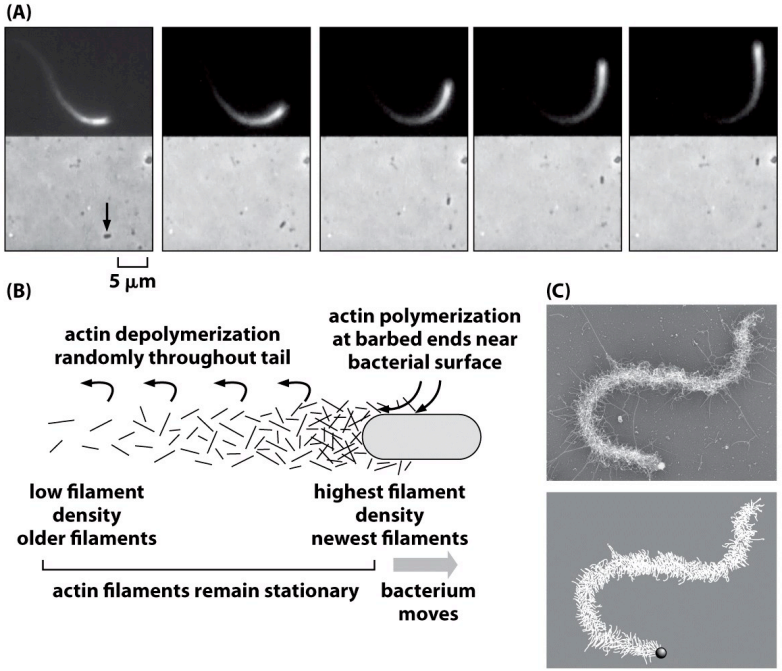

Figure 15.3 Physical Biology of the Cell (© Garland Science 2009)

How is polymerization controlled in space and time?

- ***Just as with the measurement of cell growth described earlier, bulk growth assays using light absorption (or fluorescence) as a readout have spoken volumes on mechanism.***
- ***One of the outcomes of such experiments is the discovery of molecules that nucleate polymerization of new filaments (or branches off of existing filaments).***
- ***Using these experiments, they proved the existence of protein nucleating factors.***

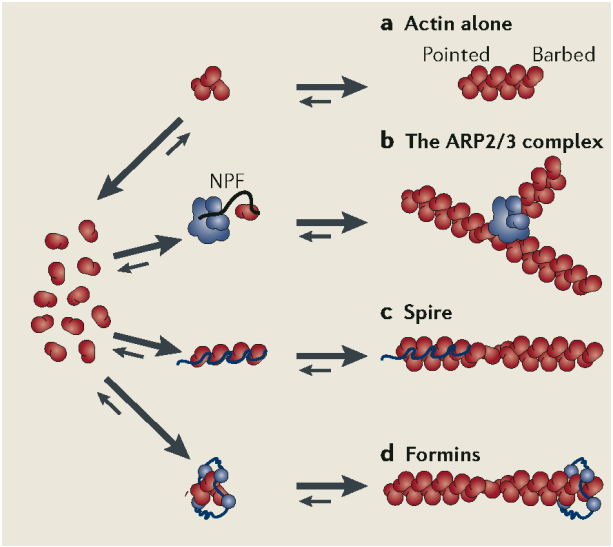

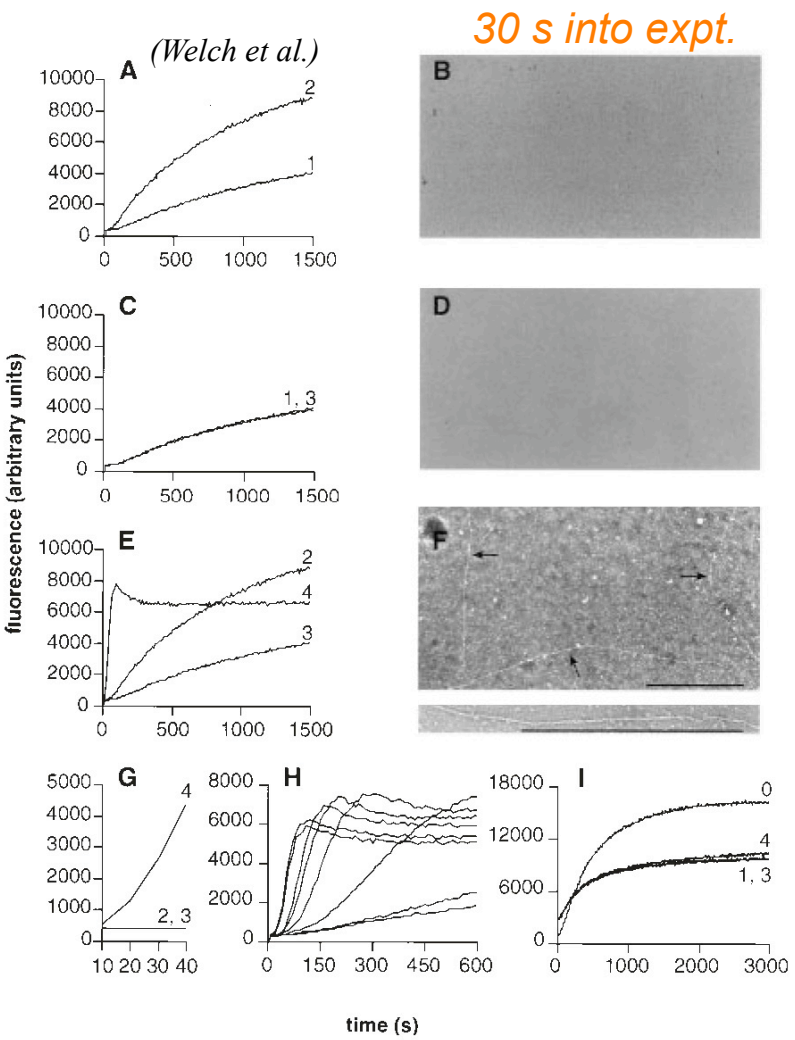

THE CONTROL OF ACTIN POLYMERIZATION AT THE LEADING EDGE

- ***Spacetime control of polymerization is mediated by a host of different proteins that do stuff such as: cap, nucleate, branch, sequester, etc. the actin itself.***
- ***Our story will focus on one little piece of this complex system, namely, the way in which Arp2/3 leads to the synthesis of new filaments.***
- ***Key point: signal integration – how do cells know when and where to put in new actin filaments?***

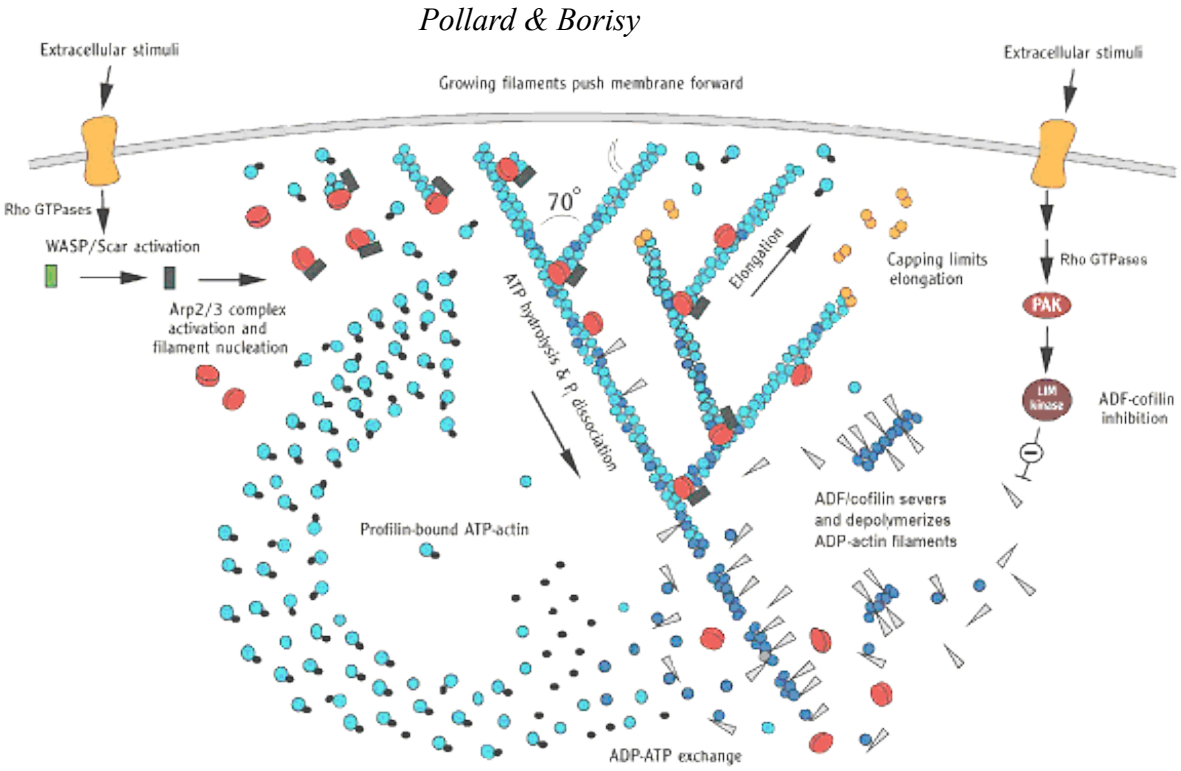

SIGNALING AND POLYMERIZATION

- ***External signals activate Arp2/3 which in turn nucleates actin polymerization.***
- ***Group of Wendell Lim has used a Lego approach to mix and match components so that signals normally reserved for other circuits can induce polymerization.***
- ***Do we really "understand" how these molecules work? Let theory and predictions be the judge of that!***

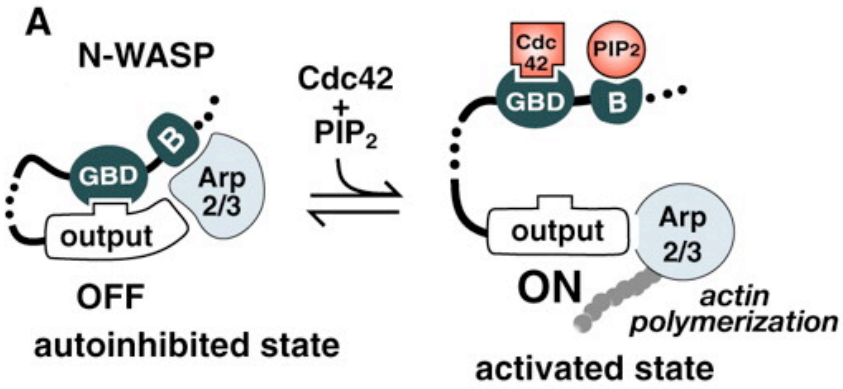

(Lim et al., Science)

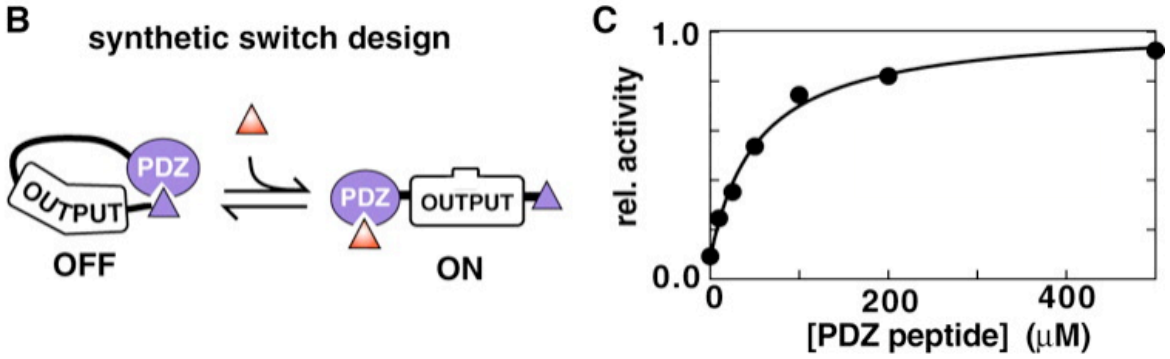

COMPUTING THE ACTIVITY OF THE SWITCH

- ***Competition between tethered ligand and free ligands.***
- ***Use simple ideas from statistical mechanics to reckon the free energy of the various contributions.***

STATE	ENERGY	MULTIPLICITY	BOLTZMANN WEIGHT
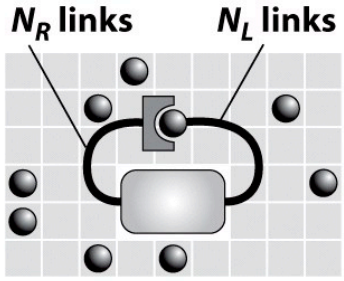	$\varepsilon_b + L\varepsilon_{sol}$	$\frac{\Omega!}{L!(\Omega-L)!}\,\frac{(N_R+N_L)!}{\left(\left(\frac{N_R+N_L}{2}\right)!\right)^2}$	$e^{-\beta L\varepsilon_{sol}}e^{-\beta\varepsilon_b}$
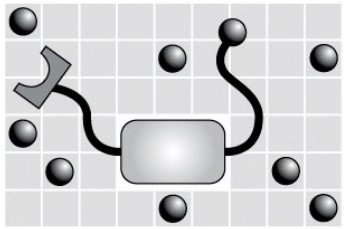	$L\varepsilon_{sol}$	$\frac{\Omega!}{L!(\Omega-L)!}\,2^{N_R}2^{N_L}$	$e^{-\beta L\varepsilon_{sol}}$
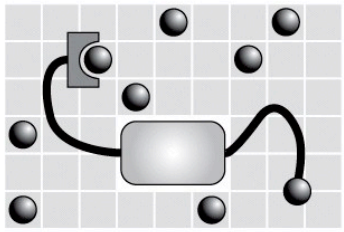	$\varepsilon_b + (L-1)\varepsilon_{sol}$	$\frac{\Omega!}{(L-1)!(\Omega-(L-1))!}\,2^{N_R}2^{N_L}$	$e^{-\beta(L-1)\varepsilon_{sol}}e^{-\beta\varepsilon_b}$

Figure 19.37 Physical Biology of the Cell (© Garland Science 2009)

TUNING TETHERS TO ALTER SIGNALING

- *We view the tether length as a dial that can be tuned in order to vary the probability that N-Wasp will activate Arp2/3.*
- *As with many free energy stories, the point here is a competition between the free and tethered ligands and their entropies (especially).*

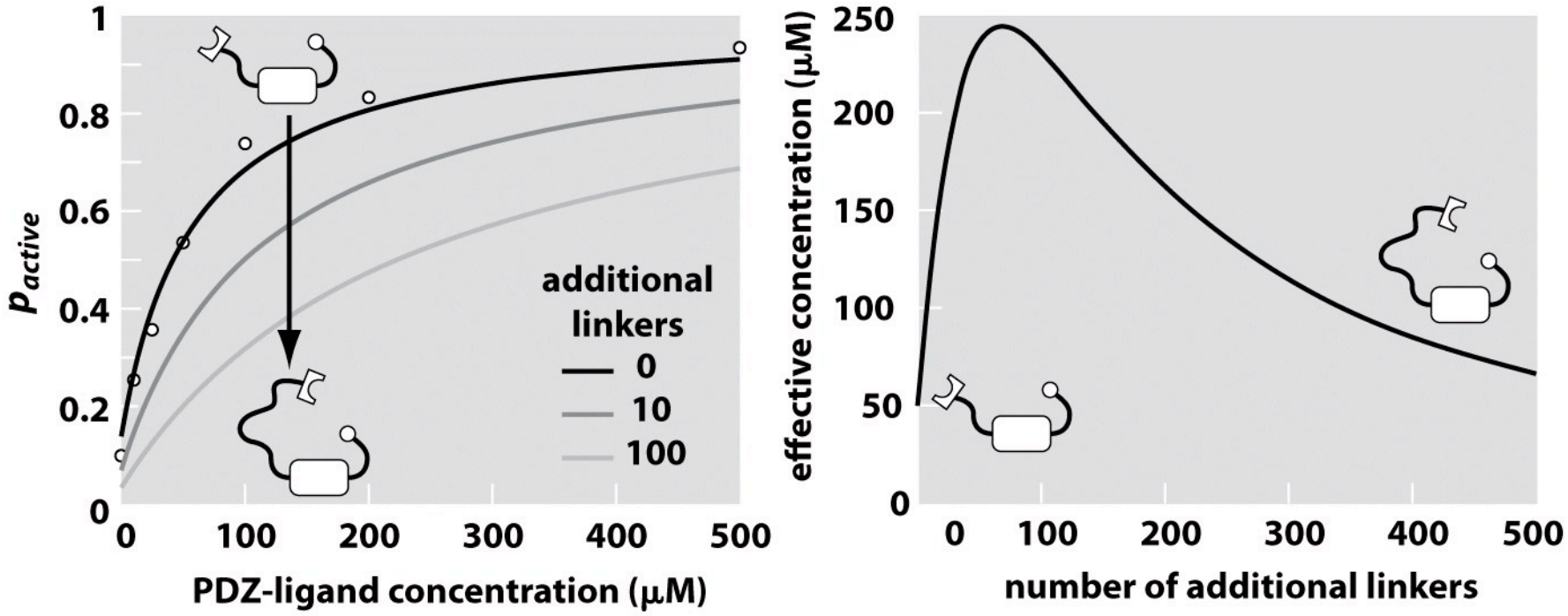

Figure 19.39 Physical Biology of the Cell (© Garland Science 2009)